Equivalence between C^1-continuous Cubic B-splines and Cubic Hermite Polynomials in Finite Element and Collocation Methods

CHRISTOPHER G. PROVATIDIS
School of Mechanical Engineering,
National Technical University of Athens,
9 Iroon Polytechniou, 157 80 Zografou,
GREECE

Abstract: - In this paper, we will show that the C^1-continuous B-spline functional set of polynomial degree $p=3$, can be written as a linear transformation of the well-known piecewise cubic Hermite polynomials. This change of functional basis means that the global B-spline finite element solution is equivalent to that of usual piecewise finite elements in conjunction with cubic Hermite polynomials, with two degrees per nodal point, like those used in beam-bending analysis. In this context, we validate the equivalence between the global B-spline solution and the piecewise solution in boundary-value and eigenvalue problems, for collocation and Ritz-Galerkin methods.

Key-Words: - Finite element method, Ritz-Galerkin method, Collocation method, B-spline, Hermite polynomials, Knot insertion, Bézier extraction, wave equation, Boundary-value problem, Computational mechanics.

Received: June 21, 2024. Revised: December 11, 2024. Accepted: December 28, 2024. Published: December 31, 2024.

1 Introduction

The use of splines dates to the early days of shipbuilding and engineering. Splines were originally flexible strips of wood or metal used by shipbuilders and draftsmen to draw smooth, curved lines between fixed points. This practice likely originated in the 18th century, with splines being essential for creating the accurate, smooth curves needed in hull designs and other structural elements.

The mathematical formalization of "B-splines" as smooth, piecewise-polynomial functions can be traced back to 1946, [1]. In the beginning, B-splines were defined using uncomfortable truncated powers but, later in 1966, B-splines were re-defined in terms of bell-shaped basis functions associated with control points or coefficients [2], as we know them today.

One of the first publications on the implementation of B-splines in the numerical solution of ordinary (ODE) and partial differential equations (PDEs) is [3]. Later, a fast method was proposed to calculate B-splines and their derivatives by recursion [4], and this is the standard technique applied to this date.

Regarding the numerical solution of ODEs and PDEs, B-splines were implemented initially in conjunction with the Collocation method [5] and later the Finite element method [6].

In the B-spline *collocation* method, it was found that the polynomial degree $p=3$ in conjunction with C^1-continuity (i.e., double inner knots) is ideal, because if two collocation points are taken between two successive fixed points (knots), they create so many equations as the number of the unknowns. The ideal position for these two collocation points is the image of the Gauss points, [7].

In the B-spline *finite element* method, the standard is to use basis functions of C^2-continuity (i.e., single inner knots) [6]. Nevertheless, when an elastic continuum is coupled with beams or plates, rotational degrees of freedom (DOF) appear, and thus more than two DOF $(u,\partial u/\partial x)$ may be associated with each nodal point. This in turn suggests the utilization of C^1-continuity approximation of the displacement field, [8].

In this paper, we shall show that despite the global character of the C^1-continuous cubic B-spline approximation, there is an inherent linear relationship between this functional basis and the four cubic Hermite polynomials (local approximation) in the interior of the knot spans. This in turn explains the coincidence of the numerical results which were obtained using the global and local approximations, in both the collocation and the Ritz-Galerkin formulations, [8].

2 Global and Local Approximations

2.1 Global Approximation (B-spline)

Based on a set of fixed points, $\{x_1, x_2, \ldots, x_{\tilde{n}-1}, x_{\tilde{n}}\}$, and considering a certain multiplicity λ for the inner points $\{x_2, \ldots, x_{\tilde{n}-1}\}$ while the multiplicity at the ends $(x_1, x_{\tilde{n}})$ is usually standardized at $p+1$, we can construct the so-called *knot vector* U.

For example, in the case of four uniform cubic B-spline elements, where the fixed points are $\{x_1, x_2, x_3, x_4, x_5\} = \{0, 1/4, 1/2, 3/4, 1\}$, i.e. $\tilde{n}=5$ fixed points, taking double inner knots $(\lambda=2)$, the knot vector becomes:

$$U=\left\{0,0,0,0,\frac{1}{4},\frac{1}{4},\frac{1}{2},\frac{1}{2},\frac{3}{4},\frac{3}{4},1,1,1,1\right\}. \quad (1)$$

If the knot vector in Eq. (1) is written in the form:

$$U=\{u_1,u_2,\ldots,u_m\}, \quad (2)$$

the number of the involved basis functions will be:

$$n=m-(p+1). \quad (3)$$

Therefore, since $m=14$ and $p=3$, the above knot vector gives $n=14-(3+1)=10$, i.e., ten C^1-continuous basis functions which are shown in Figure 1.

2.1.1 Galerkin Method

In the Ritz-Galerkin formulation dealing with the above knot vector *U*, where double inner knots have been considered, the numerical solution $u(x)$ is approximated as a series of all these ten basis functions. In general, we have:

$$u(x)=\sum_{i=1}^{n} N_i(x)\alpha_i\,, \quad (4)$$

where $N_i(x)$ are the B-spline (basis) functions and α_i the generalized coefficients (DOFs: degrees of freedom) to be determined. To determine $N_i(x)$, one possibility is to use the MATLAB® function `spcol`.

Within each of the $(\tilde{n}-1)$ fixed-point spans (i.e. $[x_1,x_2],[x_2,x_3],\ldots,[x_{\tilde{n}-1},x_{\tilde{n}}]$), there are only $(p+1)$ non-zero basis functions (local support property), and thus we usually refer to $(\tilde{n}-1)$ B-spline elements. Each of these B-spline elements is treated in a similar way with the conventional finite element method. To make this issue clear, we resort to a typical partial differential equation such as the one-dimensional wave equation in the interval $[0,L]$:

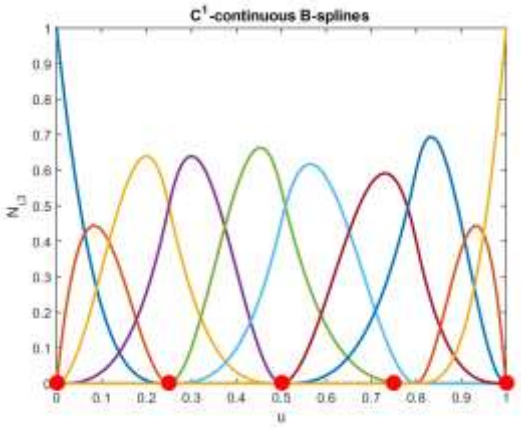

Fig. 1: Basis functions for C^1-continuity of inner knots

$$\frac{1}{c^2}\frac{\partial^2 u}{\partial t^2}-\frac{\partial^2 u}{\partial x^2}=0\,, \quad (5)$$

which by virtue of Eq. (4) leads to the well-known matrix form:

$$[\mathbf{M}]\{\ddot{\mathbf{u}}(t)\}+[\mathbf{K}]\{\mathbf{u}(t)\}=\{\mathbf{f}(t)\}\,, \quad (6)$$

with

$$[\mathbf{M}]_{ij}=\frac{1}{c^2}\int_0^L N_i N_j \mathrm{d}x \quad \text{and} \quad [\mathbf{K}]_{ij}=\int_0^L N_i' N_j' \mathrm{d}x\,, \quad (7)$$

Although the integrals in Eq. (7) refer to the entire domain [0, *L*], the piecewise character of B-splines makes it necessary to perform numerical integration within the $(\tilde{n}-1)$ B-spline elements, i.e. in the four ones of the example corresponding to the knot vector of Eq. (1), considering the local support property. In more detail, since $p=3$, in the first element [0,1/4] the nonzero basis functions will be $\{N_1, N_2, N_3, N_4\}$, in the second will be $\{N_3, N_4, N_5, N_6\}$, in the third will be $\{N_5, N_6, N_7, N_8\}$, whereas in the fourth $\{N_7, N_8, N_9, N_{10}\}$.

In general, since the total number of DOFs is $n=2\tilde{n}$, the produced stiffness matrix will be of size $n\times n=2\tilde{n}\times 2\tilde{n}$. Furthermore, imposing the two boundary conditions (BCs), the number of equations reduces to $n_{eq}=2(\tilde{n}-1)$, which is in consistency with the unknown DOFs associated to the $(\tilde{n}-2)$ nodal points in the interior plus one DOF per end. For example, the matrices associated to Eq. (1) are of size 10 × 10, while after the imposition of the BCs the deleted ones become of size 8 × 8, i.e. we have eight equations and eight unknowns, which is a straightforward case.

Note that since the polynomial degree is $p=3$, according to Eq. (7) the maximum polynomial degree involved in the integrands is $2p=6$, and thus for accurate numerical integration the required number of Gauss points per element will be $n_g=4$.

2.1.2 Collocation Method

Similarly, in the Collocation formulation using the same global cubic polynomials $N_i(x)$ which were created considering the multiplicity of inner knots equal $\lambda=2$, the abovementioned discrete breakpoints $x_1, x_2, \ldots, x_{\tilde{n}}$ create the abovementioned $(\tilde{n}-1)$ B-spline elements. Now, considering two collocation points per element (preferably at the Gauss points as proposed in [7]), we derive $n_{eq}=2(\tilde{n}-1)$ equations, which is the same number as that in the Galerkin method (see Sect. 2.1.1). If the collocation points are denoted by $x_{col}=x_j$, the governing equation of motion is again given by Eq. (6), but now we have:

$$[\mathbf{M}]_{ij}=\frac{1}{c^2}N_i\left(x_j\right) \quad \text{and} \quad [\mathbf{K}]_{ij}=-N_i''\left(x_j\right). \quad (8)$$

2.2 Local Approximation

2.2.1 Galerkin Method

In the Ritz-Galerkin formulation (i.e., the Finite Element Method), when dealing with one-dimensional (1D) problems, the computational mesh consists of the nodal points $x_1, x_2, \ldots, x_{\tilde{n}}$, which create the finite elements in the sub-intervals $[x_1, x_2]$, $[x_2, x_3]$, …, $[x_{\tilde{n}-1}, x_{\tilde{n}}]$. Considering cubic Hermite polynomials per element, the numerical solution $u(x)$ may be approximated using two degrees of freedom (DOF) per nodal point (i.e., four DOFs per cubic Hermite element). Since the total number of DOFs is $n=2\tilde{n}$, the produced stiffness matrix will be again of size $2\tilde{n}\times 2\tilde{n}$, as happened with the global formulation as well. Furthermore, imposing the two boundary conditions of Dirichlet type, the number of equations reduce to $2(\tilde{n}-1)$, which is in consistency with the unknown DOFs associated to the $(\tilde{n}-2)$ nodal points in the interior plus one DOF per end. Since the polynomial degree is $p=3$, the maximum polynomial degree in the integrands is $2p=6$, and thus the required number of Gauss points per element will be $n_g=4$, exactly as was the case in the global approximation. Nevertheless, for the wave equation, analytical expressions are possible, as shown in Appendix A.

In other words, although the local approximation uses different basis functions than what the global approximation does, the number and location of the Gaussian points are the same, and the same number of equations are derived.

2.2.2 Collocation Method

As previously happened with the global collocation, two collocation points are taken in each element, and thus $n_{eq}=2(\tilde{n}-1)$ equations are derived. In the case of two BCs of Dirichlet type, after the imposition of them, we derive a system of $n_{eq}=2(\tilde{n}-1)$ equations with the same number of unknowns.

It is worth mentioning that the equations matrix of the local collocation method is quite different than the corresponding matrix in the global collocation method of Section 2.1.2.

2.3 Handling of Dirichlet and Neumann Boundary Conditions

Now we consider one end (let it be the left one) under Dirichlet-type BC, while the BC of the other (right end) is of Neumann type. Below we discuss the difference in the handling for the two previous formulations.

2.3.1 Galerkin Method

In the Galerkin method, whatever the approximation is (global or local), we merely delete the first row (associated with the BC of Dirichlet type) in the mass and stiffness matrices. This results in $n_{eq}=2(\tilde{n}-1)$ equations and the same number of unknowns. Therefore, the numerical solution is a straightforward procedure.

2.3.2 Collocation Method

In both the global and local approximation, we have a system of $n_{eq}=2(\tilde{n}-1)$ equations and $(2\tilde{n})$ DOFs in total. Therefore, whatever the approximation is (global or local), we delete the first column (associated to the BC of Dirichlet type at the first DOF) in the mass and stiffness matrices. As a result, the remaining equations matrix becomes non-square of size $(2\tilde{n}-2)\times(2\tilde{n}-1)$, and thus we must find a way to reduce the number of columns by one. In this context, regarding the right end at which a BC of Neumann type occurs, the procedure is different for the local and the global approximation.

In more detail, in the *local* approximation the condition $\partial u/\partial x=0$ at $x=x_{\tilde{n}}=L$ is directly applicable at the n−th DOF because it is prescribed and thus the n−th (last) column must be *deleted*. Therefore, a system of $n-2=2\tilde{n}-2$ equations with $n-2=2\tilde{n}-2$ unknowns is produced.

In contrast, in the *global* approximation a more complex procedure must be followed. Since the approximate solution is given by Eq. (4) where the

n-th DOF α_n (or even its α_{n-1} due to the mirroring) does not exactly represent the derivative $\partial u/\partial x$, it is our preference to eliminate one out of the $(n-1)$ free DOFs. More accurately, taking the first derivative in both parts of Eq. (4), considering homogeneous BC of Neumann type, and then solving (say) in α_{n-1}, we have:

$$\frac{\partial u}{\partial x}=\sum_{i=1}^{n}\frac{\partial N_i(L)}{\partial x}\alpha_i=0, \tag{9}$$

and thus solving (say) in α_{n-1}, we receive:

$$\alpha_{n-1}=-\frac{1}{N'_{n-1}(L)}\sum_{\substack{i=1\\ i\neq(n-1)}}^{n}N'_i(L)\alpha_i. \tag{10}$$

In the particular case of cubic B-spline approximation (i.e., $p=3$), it can be shown that *only two* out of the four nonzero basis functions within the last element $[x_{\tilde{n}-1},x_{\tilde{n}}]$ have *nonzero derivatives* at the end point $(x=x_{\tilde{n}}=L)$. This is obviously valid for $\tilde{n}=2$ referring to a set of four Hermite functions which covers the entire domain $[0=x_1,x_2=x_{\tilde{n}}=L]$, but holds for every n.

Therefore, for $p=3$, Eq. (10) is simplified to

$$\alpha_{n-1}=-\frac{N'_n(L)}{N'_{n-1}(L)}\alpha_n. \tag{11}$$

If we return to the matrix formulation, the arbitrary $i-$th equation of motion is written as:

$$\begin{aligned}&(m_{i1}\ddot{\alpha}_1+m_{i2}\ddot{\alpha}_2+\cdots+m_{i,n-2}\ddot{\alpha}_{n-2}+m_{i,n-1}\ddot{\alpha}_{n-1}+m_{i,n}\ddot{\alpha}_n)\\&+(k_{i1}\alpha_1+k_{i2}\alpha_2+\cdots+k_{i,n-2}\alpha_{n-2}+k_{i,n-1}\alpha_{n-1}+k_{i,n}\alpha_n)\\&=f_i(t)\end{aligned} \tag{12}$$

Substituting α_{n-1} from Eq. (11) into Eq. (12), after rearrangement we receive:

$$\begin{aligned}&\left[m_{i1}\ddot{\alpha}_1+m_{i2}\ddot{\alpha}_2+\cdots+m_{i,n-2}\ddot{\alpha}_{n-2}+\left(m_{i,n}-m_{i,n-1}\frac{N'_n(L)}{N'_{n-1}(L)}\right)\ddot{\alpha}_n\right]\\&+\left[k_{i1}\alpha_1+k_{i2}\alpha_2+\cdots+k_{i,n-2}\alpha_{n-2}+\left(k_{i,n}-k_{i,n-1}\frac{N'_n(L)}{N'_{n-1}(L)}\right)\alpha_n\right]\\&=f_i(t)\end{aligned} \tag{13}$$

Equation (13) shows that the first $(n-2)$ columns in the mass and stiffness matrices must be preserved as are, while the $(n-1)$-th column must be embodied into the $n-$th column which will eventually replace the $(n-1)$-th one. More precisely, Appendix B shows that $N'_{n-1}(L)=-N'_n(L)$, and therefore the ratio involved in Eq. (13) becomes:

$$\frac{N'_n(L)}{N'_{n-1}(L)}=-1. \tag{14}$$

Therefore, by virtue of Eq. (14), one may observe that the imposition of a Neumann BC at the right end ($x=L$) imposes two equal coefficients at the end (cf. Eq. (11)), i.e. $\alpha_{n-1}=\alpha_n$. Therefore, the reduction of the number of columns by one is accomplished merely by the *addition* of the last two columns in only one column.

3 From the Knot Vector to the Hermite polynomials

Although the global basis functions shown in Figure 1 do not remind the Hermite polynomials at all, in this section we shall determine a linear relationship between the C^1-continuous B-splines and the classical Hermite polynomials.

The first step is to establish a relationship between the functional set (B-splines) of C^1 continuity and the Bernstein polynomials, which is usually called '*Bezier extraction*', [9]. This task can be easily performed by increasing the multiplicity of inners knots, from $\lambda=2$ (e.g., Eq. (1)) to $\lambda'=3$.

In general, for a knot vector such as that in Eq. (2) associated to a set of control points $\{P_1,...,P_n\}$, a knot insertion at the position $u=\bar{u}$ requires -first of all- the determination of the unique index k so as $\bar{u}\in[u_k,u_{k+1})$. Then, the control points $\{P_1,...,P_{k-p}\}$ as well as $\{P_{k+1},...,P_n\}$ remain invariable at their previous position, while p new control points Q replace the older ones according to the formula:

$$Q_{i+1}=(1-a_{i+1})P_i+a_{i+1}P_{i+1},\ \text{with}\ k-p+1\le i+1\le k, \tag{15a}$$

with,

$$a_{i+1}=\frac{\bar{u}-u_{i+1}}{u_{i+1+p}-u_{i+1}} \tag{15b}$$

If Eq. (15a) is successively applied to all the n_{in} inner knots of the vector U, we easily establish the non-square matrix $[T_2]$ (of size $n\times(n+n_{in})$) in the following linear relationship (the superscript 't' stands for transpose):

$$\{Q\}=[T_2]^t\{P\} \tag{16}$$

Moreover, since it is well known that the shape remains unaltered after knot insertion, [9], for any

parameter u we have the same image in both systems, and hence:

$$x(u)=\left\{N_{C_1}\right\}^t\{Q\} = \left\{N_{C_0}\right\}^t\{P\}, \quad (17)$$

where $\{N_{C1}\}^t$ and $\{N_{C0}\}^t$ are the transpose of the column vectors including the n basis functions of C^1-continuity (such as those shown in Figure 1) and the $n+p$ basis functions of C^0 continuity (shown in Figure 2), respectively. Obviously, the column-vector $\{N_{C0}\}^t$ coincides with the well-known column-vector of Bernstein polynomials, and thus we can write:

$$\left\{N_{C0}\right\}=\{B\}. \quad (18)$$

Clearly, for the case of the knot vector given by Eq. (1) and associated to the ten C^1-continuous basis functions shown in Figure 1, the corresponding set of thirteen C^0-continuous Bernstein polynomials (with $\{N_{C0}\}$ = $\{B\}$) is shown in Figure 2. Substituting Eq. (16) into Eq. (17), and then deleting the common factor $\{P\}$ in both parts of the equality, we receive the following linear relationship between the C^1-continuous basis functions and the C^0-continuous Bernstein polynomials:

$$\left\{N_{C1}\right\}=\left[T_2\right]\cdot\{B\}. \quad (19)$$

The next step is to express the Hermite polynomials:

$$h_{00}(u)=2u^3-3u^2+1=(1+2u)(1-u)^2, \quad (20a)$$

$$h_{10}(u)=u^3-2u^2+u=u(1-u)^2, \quad (20b)$$

$$h_{01}(u)=-2u^3+3u^2=u^2(3-2u), \quad (20c)$$

$$h_{11}(u)=u^3-u^2=u^2(u-1), \quad (20d)$$

in terms of the Bernstein-Bézier ones:

$$B_0(u)=(1-u)^3, \quad (21a)$$

$$B_1(u)=3(1-u)^2u, \quad (21b)$$

$$B_2(u)=3(1-u)u^2, \quad (21c)$$

$$B_3(u)=u^3. \quad (21d)$$

The conventional cubic Hermite polynomials are shown in Figure 3, where each node (filled by red color) is associated with two shape functions as follows. At a certain node, one of the two shape functions takes the unity value whereas the first derivative of the other equals unity.

Considering Eq. (20) and Eq. (21), one may validate the obvious linear relationships between the two functional sets, per element 'e':

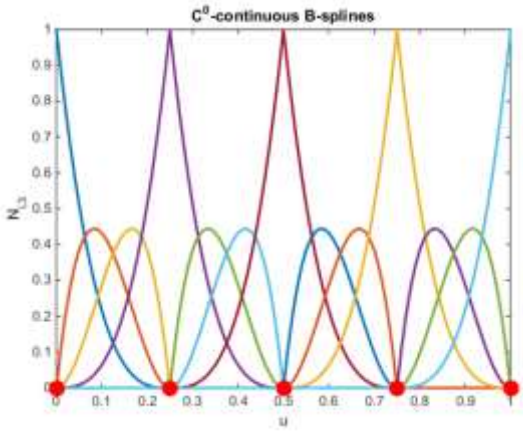

Fig. 2: Basis functions for C^0-continuity of inner knots

$$\left[H_e\right]=\begin{bmatrix}h_{00}\\h_{10}\\h_{01}\\h_{11}\end{bmatrix}=\begin{bmatrix}1&1&0&0\\0&\frac{1}{3}&0&0\\0&0&1&1\\0&0&-\frac{1}{3}&0\end{bmatrix}\cdot\begin{bmatrix}B_0\\B_1\\B_2\\B_3\end{bmatrix}, \quad (22)$$

and after inversion:

$$\left[B_e\right]=\begin{bmatrix}B_0\\B_1\\B_2\\B_3\end{bmatrix}=\begin{bmatrix}1&-3&0&0\\0&3&0&0\\0&0&0&-3\\0&0&1&3\end{bmatrix}\cdot\begin{bmatrix}h_{00}\\h_{10}\\h_{01}\\h_{11}\end{bmatrix}. \quad (23)$$

By substituting Eq. (23) into Eq. (19), we derive the desired linear relationship between the C^1 and the C^0-continuous sets of basis functions:

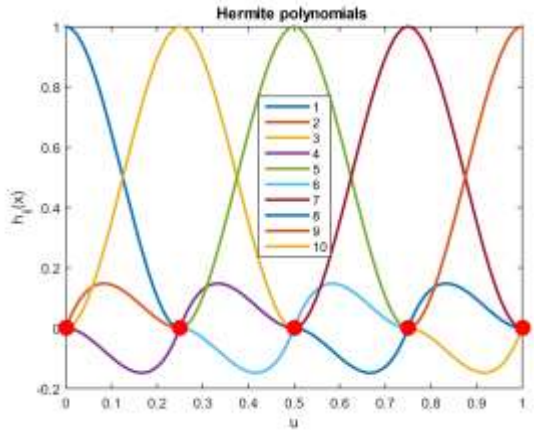

Fig. 3: Cubic Hermite polynomials

$$\left\{N_{C1}\right\}=\left(\left[T_2\right]\cdot\left[T_3\right]\right)\cdot\{H\}, \quad (24)$$

with

$$[T_3]=\begin{bmatrix}1 & -3 & 0 & 0\\ 0 & 3 & 0 & 0\\ 0 & 0 & 0 & -3\\ 0 & 0 & 1 & 3\end{bmatrix}. \quad (25)$$

In general, if we collect the partial transformations $[T_2]$ and $[T_3]$ into a total transformation matrix $[T]$ given by:

$$[T]=[T_2]\cdot[T_3], \quad (26)$$

Eq. (24) is shortened as:

$$\{N_{C1}\}=[T]\cdot\{H\}. \quad (27)$$

For the case of a knot vector U with double inner knots, we propose the following theorem which establishes an easily implemented algorithm:

THEOREM-1: Let $\{x_1,\ldots,x_{\bar{n}}\}$ be a non-decreasing sequence of single fixed points (interpolation points). Let also the point spans (i.e., the B-spline elements) be of length $l_1,\ldots,l_{\bar{n}}$. Obviously, there are $(\bar{n}-2)$ inter-element junctions x_q with $q=2,\ldots,\bar{n}-1$. The q-th junction is characterized by the ratio $\rho_q=l_q/(l_{q-1}+l_q)$, which is the length of the right point span over the length of the sum of the two adjacent elements. Show that:

- The Bézier extraction operator $[T_2]$ from C^1 to C^0-continuity is automatically produced when considering three types of elements, as follows:
  - The first element (e=1) corresponds to the matrix:

$$[T_2]_{e=1}=\begin{bmatrix}1 & 0 & 0 & 0\\ 0 & 1 & 0 & 0\\ 0 & 0 & 1 & \rho_2\\ 0 & 0 & 0 & 1-\rho_2\end{bmatrix}. \quad (28)$$

  - All intermediate elements $(e=2,\ldots,\bar{n}-2)$ correspond to the matrix:

$$[T_2]_e=\begin{bmatrix}\rho_e & 0 & 0 & 0\\ 1-\rho_e & 1 & 0 & 0\\ 0 & 0 & 1 & \rho_{e+1}\\ 0 & 0 & 0 & 1-\rho_{e+1}\end{bmatrix}. \quad (29)$$

  - The last element $(e=\bar{n}-1)$ corresponds to the matrix:

$$[T_2]_{e=\bar{n}-1}=\begin{bmatrix}\rho_{\bar{n}-1} & 0 & 0 & 0\\ 1-\rho_{\bar{n}-1} & 1 & 0 & 0\\ 0 & 0 & 1 & 0\\ 0 & 0 & 0 & 1\end{bmatrix}. \quad (30)$$

- The final transformation element matrices from B-splines of C^1-continuity to Hermite polynomials are as follows:
  - The first element (e=1) corresponds to the matrix:

$$[T]_{e=1}=\begin{bmatrix}1 & -3 & 0 & 0\\ 0 & 3 & 0 & 0\\ 0 & 0 & \rho_2 & -3(1-\rho_2)\\ 0 & 0 & -\rho_2 & 3(1-\rho_2)\end{bmatrix}. \quad (31)$$

  - All intermediate elements $(e=2,\ldots,\bar{n}-2)$ correspond to the matrix:

$$[T]_e=\begin{bmatrix}\rho_e & -3\rho_e & 0 & 0\\ 1-\rho_e & 3\rho_e & 0 & 0\\ 0 & 0 & \rho_{e+1} & -3(1-\rho_{e+1})\\ 0 & 0 & 1-\rho_{e+1} & 3(1-\rho_{e+1})\end{bmatrix}. \quad (32)$$

  - The last element $(e=\bar{n}-1)$ corresponds to the matrix:

$$[T]_{e=\bar{n}-1}=\begin{bmatrix}\rho_{\bar{n}-1} & -3\rho_{\bar{n}-1} & 0 & 0\\ 1-\rho_{\bar{n}-1} & 3\rho_{\bar{n}-1} & 0 & 0\\ 0 & 0 & 0 & -3\\ 0 & 0 & 1 & 3\end{bmatrix}. \quad (33)$$

Proof: We consider the knot vector U with double inner knots, which ensures C^1-continuity at the breakpoints. We successively apply a knot insertion at all the inner breakpoints by using Eq. (15), starting from the breakpoint x_2 till the fixed point $x_{\bar{n}-1}$. Since for a clamped curve the first four (i.e., $p+1$) knots equal zero and the multiplicity is $\lambda=2$ (hence $(p+1)+\lambda=4+2=6$), one may easily understand that the index k, so that the inserted value x_q at the k-th breakpoint belongs to the interval $[u_k,u_{k+1})$ of the knot vector before this insertion, becomes equal:

$$k=6+3(q-2)=6,9,12,\ldots \quad (34)$$

Based on the indices shown in Eq. (34), the combination of Eq. (15a) and Eq. (15b) determines that the only newly inserted control point is $Q_{k-2}=(1-a_{k-2})P_{k-1}+a_{k-2}P_{k-2}$, which is influenced by the factor:

$$a_{k-2}=\frac{x_q-u_{k-2}}{u_{k-2+p}-u_{k-2}}\text{, where } u_{k-2}=x_{q-1} \text{ and } u_{k-2+p}=x_{q+1} \tag{35a}$$

or, equivalently

$$a_{k-2}=\frac{L_{left}}{L_{left}+L_{right}}, \tag{35b}$$

where $L_{left}(\equiv l_{q-1})$ and $L_{right}(\equiv l_q)$ are the lengths of breakpoint spans at the left and at the right, respectively, of the inserted knot x_q. Therefore, we have:

$$\begin{aligned} Q_{k-2} &= (1-a_{k-2})P_{k-3}+a_{k-2}P_{k-2} \\ &= \left(1-\frac{L_{left}}{L_{left}+L_{right}}\right)P_{k-3}+\left(\frac{L_{left}}{L_{left}+L_{right}}\right)P_{k-2} \\ &= \left(\frac{L_{right}}{L_{left}+L_{right}}\right)P_{k-3}+\left(\frac{L_{left}}{L_{left}+L_{right}}\right)P_{k-2} \\ &= \rho_q P_{k-3}+(1-\rho_q)P_{k-2} \end{aligned} \tag{36}$$

Note that in each knot insertion, only one control point is revised whereas the other control points remain invariable as are. After each knot insertion, the knot vector *U* is updated by adding the value x_q in the previous one.

The above Eq. (36) is the one that successively contains the mentioned length ratios ρ_q, with $q=2,\ldots,\bar{n}-1$. The rest of the proof is straightforward and is left as an exercise to the interested reader. Several numerical validations of Theorem-1 are given in Section 5.

4 Equivalence between Global and Local Approximation

Due to the linear relationship between the two functional sets according to Eq. (27), the mass and stiffness matrices in the former system will be a quadratic form of those in the latter and vice versa. This is well known in the eigenvalue problem where the calculated eigenvalues are given by the so-called Rayleigh-Ritz quotient.

For the sake of simplicity, the relation between the two functional sets, i.e. the initial $N_P=N_{C1}$ and the final $N_Q=H$, is re-written as follows:

$$\{N_P\}=[T]\cdot\{N_Q\}, \tag{37}$$

whereas the relation between the two coefficient sets, i.e. the initial generalized $\{\alpha_P\}=\{\alpha_1,\ldots,\alpha_n\}$ and the final nodal values $\{\alpha_Q\}=\{u_1,u_1',\ldots,u_{\bar{n}},u_{\bar{n}}'\}$ will be (Eq. (16)):

$$\{\alpha_Q\}=[T]\cdot\{\alpha_P\}. \tag{38}$$

Regarding a typical ODE:

$$-\frac{d^2u}{dx^2}=b(x), \tag{39}$$

the matrix equation in the initial system will be:

$$[K]\{\alpha_P\}=\int_0^L N_P b(x)dx \tag{40}$$

where

$$[K]=\int_0^L \{N_P'\}\{N_P'\}^t\,dx, \tag{41}$$

where $\{N_P'\}$ represents the first derivative of the vector $\{N_P\}$.

Substituting $\{N_P\}$ from Eq. (37) and from Eq. (38) into Eq. (41), the latter becomes:

$$\begin{aligned} &[T]\cdot\left(\int_0^L \{N_Q'\}\{N_Q'\}^t dx\right)\cdot[T]^t([T]^t)^{-1}\cdot a_Q \\ &=[T]\cdot\int_0^L N_Q b(x)dx, \end{aligned} \tag{42}$$

whence, after deletion of the pre-multiplier [*T*], we get:

$$\left(\int_0^L \{N_Q'\}\{N_Q'\}^t dx\right)\cdot a_Q=\int_0^L N_Q b(x)dx, \tag{43}$$

Comparing Eq. (43) with the couple of Eq. (40) and Eq (41), one concludes the equivalence of the numerical solution between the initial system {*P*} (based on the C^1 continuous B-spline) and the final system {*Q*} (based on an assembly of conventional cubic Hermite elements).

Similar conclusions are derived when the mass matrix is considered as well. In both cases, the matrices of one system are quadratic forms of them in the other system, and vice versa.

5 Numerical Examples of the Transformation Matrix

In all examples of this section, we consider the unit domain [0, *L*] with *L* = 1. In the beginning, we consider uniform subdivision into n_{nele} = 2, 3, 4 cubic B-spline elements. Then, we also test a non-uniform assembly.

5.1 Two Uniform B-spline Elements

Starting from the knot vector

$$U=\left\{0,0,0,0,\frac{1}{2},\frac{1}{2},1,1,1,1\right\}, \tag{44}$$

the transformation matrix from C^1- to C^0-continuity (Bernstein polynomials) is easily found as:

$$[T_2]=\begin{bmatrix}1&0&0&0&0&0&0\\0&1&0&0&0&0&0\\0&0&1&1/2&0&0&0\\0&0&0&1/2&1&0&0\\0&0&0&0&0&1&0\\0&0&0&0&0&0&1\end{bmatrix}. \tag{45}$$

Therefore, by post-multiplying $[T_2]$ of Eq. (45) with the 4 × 4 matrix $[T_3]$ of Eq. (25), according to Eq. (26), we receive the total transformation matrix $[T]$ for each of the two elements (the first e = 1, and the second e = 2):

For e = 1:

$$[T]=\begin{bmatrix}1&0&0&0\\0&1&0&0\\0&0&1&1/2\\0&0&0&1/2\end{bmatrix}\begin{bmatrix}1&-3&0&0\\0&3&0&0\\0&0&0&-3\\0&0&1&3\end{bmatrix}=\begin{bmatrix}1&-3&0&0\\0&3&0&0\\0&0&1/2&-3/2\\0&0&1/2&3/2\end{bmatrix} \tag{46a}$$

For e = 2:

$$[T]=\begin{bmatrix}1/2&0&0&0\\1/2&1&0&0\\0&0&1&0\\0&0&0&1\end{bmatrix}\begin{bmatrix}1&-3&0&0\\0&3&0&0\\0&0&0&-3\\0&0&1&3\end{bmatrix}=\begin{bmatrix}1/2&-3/2&0&0\\1/2&3/2&0&0\\0&0&1&-3\\0&0&1&3\end{bmatrix} \tag{46b}$$

Since $\rho_2=1/2$, one may validate that Eq. (46a) is according to Eq. (31), while Eq. (46b) is according to Eq. (33), as anticipated.

5.2 Three uniform B-spline Elements

We continue with the knot vector:

$$U=\left\{0,0,0,0,\frac{1}{3},\frac{1}{3},\frac{2}{3},\frac{2}{3},1,1,1,1\right\}. \tag{47}$$

In this case the transformation matrix from C^1- to C^0-continuity (in terms of Bernstein polynomials) is found to be:

$$[T_2]=\begin{bmatrix}1&0&0&0&0&0&0&0&0&0\\0&1&0&0&0&0&0&0&0&0\\0&0&1&1/2&0&0&0&0&0&0\\0&0&0&1/2&1&0&0&0&0&0\\0&0&0&0&0&1&1/2&0&0&0\\0&0&0&0&0&0&1/2&1&0&0\\0&0&0&0&0&0&0&0&1&0\\0&0&0&0&0&0&0&0&0&1\end{bmatrix} \tag{48}$$

Therefore, by multiplying Eq. (45) with the 4 × 4 matrix $[T_3]$ given by Eq. (25), we receive the transformation matrices for each of the three elements (the first e = 1, the second e = 2, and the third e = 3) which relate the four element basis functions of C^1-continuity which the four element Hermite polynomials $[h_{00}, h_{10}, h_{01}, h_{11}]$t:

For $e=1$:

$$[T]=\begin{bmatrix}1&0&0&0\\0&1&0&0\\0&0&1&1/2\\0&0&0&1/2\end{bmatrix}\begin{bmatrix}1&-3&0&0\\0&3&0&0\\0&0&0&-3\\0&0&1&3\end{bmatrix}=\begin{bmatrix}1&-3&0&0\\0&3&0&0\\0&0&1/2&-3/2\\0&0&1/2&3/2\end{bmatrix} \tag{49a}$$

For $e=2$:

$$[T]=\begin{bmatrix}1/2&0&0&0\\1/2&1&0&0\\0&0&1&1/2\\0&0&0&1/2\end{bmatrix}\begin{bmatrix}1&-3&0&0\\0&3&0&0\\0&0&0&-3\\0&0&1&3\end{bmatrix}=\begin{bmatrix}1/2&-3/2&0&0\\1/2&3/2&0&0\\0&0&1/2&-3/2\\0&0&1/2&3/2\end{bmatrix} \tag{49b}$$

For $e=3$:

$$[T]=\begin{bmatrix}1/2&0&0&0\\1/2&1&0&0\\0&0&1&0\\0&0&0&1\end{bmatrix}\begin{bmatrix}1&-3&0&0\\0&3&0&0\\0&0&0&-3\\0&0&1&3\end{bmatrix}=\begin{bmatrix}1/2&-3/2&0&0\\1/2&3/2&0&0\\0&0&0&-3\\0&0&1&3\end{bmatrix} \tag{49c}$$

One may observe that Eq. (49) has matrices of the same pattern as Eq. (46). In more detail, the transformation matrix associated with the first and the last elements is one the mirror of the other, while the upper half of the intermediate matrix (for e = 2 is the same with the lower half of the element e = 1 and the lower half of e = 2 is the same as the upper part of element e = 3). Overall, Eq. 49(a,b,c) are according to Eq. (31), Eq. (32) and Eq. (33), respectively.

5.3 Four Uniform B-spline Elements

The straightforward way is to consider the knot vector:

$$U=\left\{0,0,0,0,\underset{\lambda=2}{\frac{1}{4}},\underset{\lambda=2}{\frac{1}{4}},\underset{\lambda=2}{\frac{2}{4}},\underset{\lambda=2}{\frac{2}{4}},\underset{\lambda=2}{\frac{3}{4}},\underset{\lambda=2}{\frac{3}{4}},1,1,1,1\right\}. \tag{50}$$

Working as previously, the transformation matrix $[T_2]$ from C^1 to C^0 continuity was found as:

$$[T_2]=\begin{bmatrix} 1 & 0 & 0 & 0 & 0 & 0 & 0 & 0 & 0 & 0 & 0 & 0 & 0 \\ 0 & 1 & 0 & 0 & 0 & 0 & 0 & 0 & 0 & 0 & 0 & 0 & 0 \\ 0 & 0 & 1 & 1/2 & 0 & 0 & 0 & 0 & 0 & 0 & 0 & 0 & 0 \\ 0 & 0 & 0 & 1/2 & 1 & 0 & 0 & 0 & 0 & 0 & 0 & 0 & 0 \\ 0 & 0 & 0 & 0 & 0 & 1 & 1/2 & 0 & 0 & 0 & 0 & 0 & 0 \\ 0 & 0 & 0 & 0 & 0 & 0 & 1/2 & 1 & 0 & 0 & 0 & 0 & 0 \\ 0 & 0 & 0 & 0 & 0 & 0 & 0 & 0 & 1 & 1/2 & 0 & 0 & 0 \\ 0 & 0 & 0 & 0 & 0 & 0 & 0 & 0 & 0 & 1/2 & 1 & 0 & 0 \\ 0 & 0 & 0 & 0 & 0 & 0 & 0 & 0 & 0 & 0 & 0 & 1 & 0 \\ 0 & 0 & 0 & 0 & 0 & 0 & 0 & 0 & 0 & 0 & 0 & 0 & 1 \end{bmatrix} \quad (51)$$

Splitting the matrix $[T_2]$ (of size 10×13) into four element sub-matrices and then multiplying by the standard matrix $[T_3]$ of Eq. (25), we receive the C^1-continuous basis functions per element in terms of the corresponding Hermite polynomials of the same elements, as follows:

$$\text{For } e=1: \begin{bmatrix} N_1 \\ N_2 \\ N_3 \\ N_4 \end{bmatrix}_{C1} = \begin{bmatrix} 1 & -3 & 0 & 0 \\ 0 & 3 & 0 & 0 \\ 0 & 0 & 1/2 & -3/2 \\ 0 & 0 & 1/2 & 3/2 \end{bmatrix} . \begin{bmatrix} h_{00} \\ h_{10} \\ h_{01} \\ h_{11} \end{bmatrix}_{e=1} \quad (52a)$$

$$\text{For } e=2: \begin{bmatrix} N_3 \\ N_4 \\ N_5 \\ N_6 \end{bmatrix}_{C1} = \begin{bmatrix} 1/2 & -3/2 & 0 & 0 \\ 1/2 & 3/2 & 0 & 0 \\ 0 & 0 & 1/2 & -3/2 \\ 0 & 0 & 1/2 & 3/2 \end{bmatrix} . \begin{bmatrix} h_{00} \\ h_{10} \\ h_{01} \\ h_{11} \end{bmatrix}_{e=2} \quad (52b)$$

$$\text{For } e=3: \begin{bmatrix} N_5 \\ N_6 \\ N_7 \\ N_8 \end{bmatrix}_{C1} = \begin{bmatrix} 1/2 & -3/2 & 0 & 0 \\ 1/2 & 3/2 & 0 & 0 \\ 0 & 0 & 1/2 & -3/2 \\ 0 & 0 & 1/2 & 3/2 \end{bmatrix} . \begin{bmatrix} h_{00} \\ h_{10} \\ h_{01} \\ h_{11} \end{bmatrix}_{e=3} \quad (52c)$$

$$\text{For } e=4: \begin{bmatrix} N_7 \\ N_8 \\ N_9 \\ N_{10} \end{bmatrix}_{C1} = \begin{bmatrix} 1/2 & -3/2 & 0 & 0 \\ 1/2 & 3/2 & 0 & 0 \\ 0 & 0 & 0 & -3 \\ 0 & 0 & 1 & 3 \end{bmatrix} . \begin{bmatrix} h_{00} \\ h_{10} \\ h_{01} \\ h_{11} \end{bmatrix}_{e=4} \quad (52d)$$

One may observe that:

- The element transformation matrices in Eq. (52) are in full accordance with Eq. (49), and therefore one could blindly repeat them.
- The above transformation matrices of Eq. (52) are in full accordance with the Theorem-1 of section 3.

It is noted that the above remarks were the *inspiration* point for expressing the generally applicable Theorem-1, which is cited in section 3.

5.4 Four non-uniform B-spline Elements

In contrast to the uniform elements which are fully described in subsection 5.3, in general the transformation element matrices associated with the junction of two unequal B-spline elements differ from the standard algorithm shown in the previous section.

For example, let us continue with the non-uniform knot vector:

$$U=\left\{0,0,0,0,\frac{1}{4},\frac{1}{4},\frac{2}{4},\frac{2}{4},\frac{4}{5},\frac{4}{5},1,1,1,1\right\}. \quad (53)$$

In this case, the transformation matrix from C^1- to C^0-continuity was found to be:

$$[T_2]=\begin{bmatrix} 1 & 0 & 0 & 0 & 0 & 0 & 0 & 0 & 0 & 0 & 0 & 0 & 0 \\ 0 & 1 & 0 & 0 & 0 & 0 & 0 & 0 & 0 & 0 & 0 & 0 & 0 \\ 0 & 0 & 1 & 1/2 & 0 & 0 & 0 & 0 & 0 & 0 & 0 & 0 & 0 \\ 0 & 0 & 0 & 1/2 & 1 & 0 & 0 & 0 & 0 & 0 & 0 & 0 & 0 \\ 0 & 0 & 0 & 0 & 0 & 1 & 6/11 & 0 & 0 & 0 & 0 & 0 & 0 \\ 0 & 0 & 0 & 0 & 0 & 0 & 5/11 & 1 & 0 & 0 & 0 & 0 & 0 \\ 0 & 0 & 0 & 0 & 0 & 0 & 0 & 0 & 1 & 2/5 & 0 & 0 & 0 \\ 0 & 0 & 0 & 0 & 0 & 0 & 0 & 0 & 0 & 3/5 & 1 & 0 & 0 \\ 0 & 0 & 0 & 0 & 0 & 0 & 0 & 0 & 0 & 0 & 0 & 1 & 0 \\ 0 & 0 & 0 & 0 & 0 & 0 & 0 & 0 & 0 & 0 & 0 & 0 & 1 \end{bmatrix} \quad (54)$$

Comparing Eq. (54) to Eq. (51), one may observe that the first element remains intact (because the first two elements are of the same length equal to 0.25), the second element differs at its ends (where the two vertically placed values of 1/2 change to vertically placed values 6/11 and 5/11, respectively), and similarly the ends of the third element change (the two values of 1/2 change to 2/5 and 3/5, respectively). Obviously, the beginning of the fourth element follows the change at the end of the previous third element.

Based on the transformation matrix of Eq. (54) and writing for each of the four B-spline elements the analogous equalities such as those in Eq. (52), we receive:

$$\text{For } e=1: \begin{bmatrix} N_1 \\ N_2 \\ N_3 \\ N_4 \end{bmatrix}_{C1} = \begin{bmatrix} 1 & -3 & 0 & 0 \\ 0 & 3 & 0 & 0 \\ 0 & 0 & 1/2 & -3/2 \\ 0 & 0 & 1/2 & 3/2 \end{bmatrix} . \begin{bmatrix} h_{00} \\ h_{10} \\ h_{01} \\ h_{11} \end{bmatrix}_{e=1} \quad (55a)$$

$$\text{For } e=2: \begin{bmatrix} N_3 \\ N_4 \\ N_5 \\ N_6 \end{bmatrix}_{C1} = \begin{bmatrix} 1/2 & -3/2 & 0 & 0 \\ 1/2 & 3/2 & 0 & 0 \\ 0 & 0 & 6/11 & -15/11 \\ 0 & 0 & 5/11 & 15/11 \end{bmatrix} . \begin{bmatrix} h_{00} \\ h_{10} \\ h_{01} \\ h_{11} \end{bmatrix}_{e=2} \quad (55b)$$

$$\text{For } e=3: \begin{bmatrix} N_5 \\ N_6 \\ N_7 \\ N_8 \end{bmatrix}_{C1} = \begin{bmatrix} 6/11 & -18/11 & 0 & 0 \\ 5/11 & 18/11 & 0 & 0 \\ 0 & 0 & 2/5 & -9/5 \\ 0 & 0 & 3/5 & 9/5 \end{bmatrix} . \begin{bmatrix} h_{00} \\ h_{10} \\ h_{01} \\ h_{11} \end{bmatrix}_{e=3} \quad (55c)$$

$$\text{For } e=4: \begin{bmatrix} N_7 \\ N_8 \\ N_9 \\ N_{10} \end{bmatrix}_{C1} = \begin{bmatrix} 2/5 & -6/5 & 0 & 0 \\ 3/5 & 6/5 & 0 & 0 \\ 0 & 0 & 0 & -3 \\ 0 & 0 & 1 & 3 \end{bmatrix} . \begin{bmatrix} h_{00} \\ h_{10} \\ h_{01} \\ h_{11} \end{bmatrix}_{e=4} \quad (55d)$$

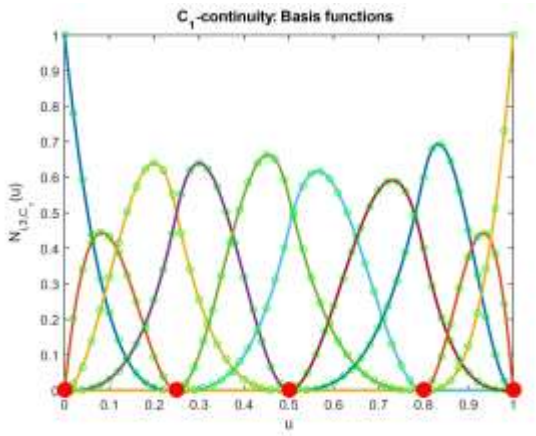

Fig. 4: Validated basis functions for C[1]-continuity of inner knots ($\lambda = 2$)

Furthermore, it was found that the original ten C^1-continuous basis functions, calculated using the `spcol` function of MATLAB®, coincide with those found by Eq. (55), as shown in Figure 4.

Rule-of-Thumb: As previously mentioned, comparing Eq. (54) with Eq. (51), the only difference concerns the double values of '1/2' which appear in the 4th, 7th, and 10th matrix columns in Eq. (51), while two pairs of them are different in Eq. (54). A careful reader may observe that each of these pairs is proportional to the ratio of the two adjacent elements while their sum equals unity. Indeed, regarding the breakpoint at $x = 0.50$ which joints the element at left ($0.25 < x < 0.50$ of length $L_{left} = 0.25$) and the element at right ($0.50 < x < 0.80$ of length $L_{right} = 0.30$), we have:

$$(T_2)_{5,7} = \frac{L_{right}}{L_{left} + L_{right}} = \frac{0.30}{0.25 + 0.30} = \frac{6}{11} \qquad (56a)$$

$$(T_2)_{6,7} = \frac{L_{left}}{L_{left} + L_{right}} = \frac{0.25}{0.25 + 0.30} = \frac{5}{11}, \qquad (56b)$$

which are exactly the elements $(T_2)_{5,7}$ and $(T_2)_{6,7}$ in the matrix $[T_2]$ of Eq. (54).

Similarly, regarding the breakpoint at $x = 0.80$, which joints the element at left ($0.50 < x < 0.80$ of length $L_{left} = 0.30$) and the element at right ($0.80 < x < 1.00$ of length $L_{right} = 0.20$), we have:

$$(T_2)_{7,10} = \frac{L_{right}}{L_{left} + L_{right}} = \frac{0.20}{0.30 + 0.20} = \frac{2}{5} \qquad (57a)$$

$$(T_2)_{8,10} = \frac{L_{left}}{L_{left} + L_{right}} = \frac{0.30}{0.30 + 0.20} = \frac{3}{5}, \qquad (57b)$$

which are exactly the elements $(T_2)_{7,10}$ and $(T_2)_{8,10}$ in the matrix $[T_2]$ of Eq. (54).

After the above discussion, the algorithm for the automatic construction of the transformation matrix $[T_2]$ is obvious. The new concept came from numerical experimentation and intuition, but rigorous proof is in Theorem-1 of Section 3.

5.5 Knots Following an Arithmetic Progression

As a final test of the proposed algorithm which uses the length ratios of the adjacent knot spans, we test the case in which the knots follow an arithmetic progression, i.e., the knot vector is:

$$U = \left[0,0,0,0,\ \underbrace{0.1,0.1}_{\lambda=2},\ \underbrace{0.3,0.3}_{\lambda=2},\ \underbrace{0.6,0.6}_{\lambda=2},\ 1,1,1,1 \right] \qquad (58)$$

Considering the three elements junctions, the corresponding length ratios (right : total) will be:

$$\rho_1 = \frac{0.3-0.1}{0.3-0.0} = \frac{2}{3},\ \rho_2 = \frac{0.6-0.3}{0.6-0.1} = \frac{3}{5},\quad \rho_3 = \frac{1.0-0.6}{1.0-0.3} = \frac{4}{7}. \qquad (59)$$

As a result, the associated transformation matrix becomes:

$$[T_2] = \begin{bmatrix} 1 & 0 & 0 & 0 & 0 & 0 & 0 & 0 & 0 & 0 & 0 & 0 & 0 \\ 0 & 1 & 0 & 0 & 0 & 0 & 0 & 0 & 0 & 0 & 0 & 0 & 0 \\ 0 & 0 & 1 & 1/2 & 0 & 0 & 0 & 0 & 0 & 0 & 0 & 0 & 0 \\ 0 & 0 & 0 & 1/2 & 1 & 0 & 0 & 0 & 0 & 0 & 0 & 0 & 0 \\ 0 & 0 & 0 & 0 & 0 & 1 & 6/11 & 0 & 0 & 0 & 0 & 0 & 0 \\ 0 & 0 & 0 & 0 & 0 & 0 & 5/11 & 1 & 0 & 0 & 0 & 0 & 0 \\ 0 & 0 & 0 & 0 & 0 & 0 & 0 & 0 & 1 & 2/5 & 0 & 0 & 0 \\ 0 & 0 & 0 & 0 & 0 & 0 & 0 & 0 & 0 & 3/5 & 1 & 0 & 0 \\ 0 & 0 & 0 & 0 & 0 & 0 & 0 & 0 & 0 & 0 & 0 & 1 & 0 \\ 0 & 0 & 0 & 0 & 0 & 0 & 0 & 0 & 0 & 0 & 0 & 0 & 1 \end{bmatrix} \qquad (60)$$

Following the same procedure as previously, the original C^1-continuous basis functions and their validation using Eq. (60) is shown in Figure 5.

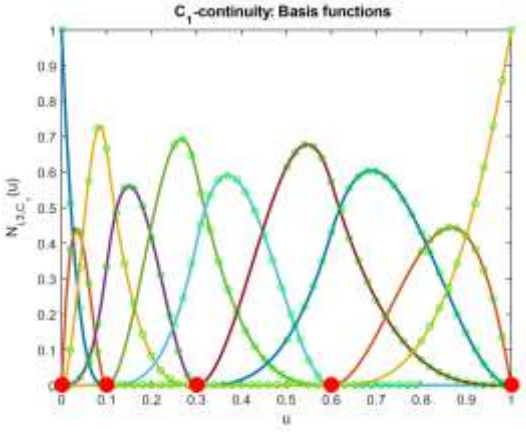

Fig. 5: Validated basis functions for C[1]-continuity of inner knots in arithmetic progression ($\lambda = 2$)

6 Boundary-Value and Eigenvalue Examples

Although the established linear relationship between the basis functions in (i) the original B-spline approximation of C^1-continuty of degree $p=3$ and (ii) the local cubic Hermite, ensures the equivalence in the solution of the BV and eigenvalue problem, we also validate this fact by a few numerical results.

6.1 Example 1: Eigenvalue Extraction

An acoustic pipe of length L, governed by the PDE of Eq. (5), is under free-free (Neumann) boundary conditions. Implementing the Galerkin and the collocation formulations, calculate some of the lowest eigenvalues, of which the exact values are given by the formula:

$$\lambda_n = \pi^2 c^2 \left(\frac{n}{L}\right)^2, \quad n=0,1,2,\ldots \tag{61}$$

Following the procedures discussed in Section 2, using four uniform elements ($n_{ele}=4$) which span the domain [0, L] according to Eq. (1), and thus having the ten basis functions shown in Figure 1, the lowest calculated eigenvalues are shown in Table 1.

One may observe that in each formulation (Galerkin or Collocation), the global and local cubic approximations lead to the *same* numerical result although each method has its own different matrices, as predicted by the preceding theory.

Table 1. Errors of calculated eigenvalues

Mode (n)	Error in percent (%)				Exact $(\lambda_n=\omega_n^2)$
	Galerkin method		Collocation method		
	Global	Local	Global	Local	
1	-	-	-	-	0.0000000e+00
2	0.00	0.00	0.02	0.02	9.8696044e+00
3	0.02	0.02	0.23	0.23	3.9478418e+01
4	0.17	0.17	0.67	0.67	8.8826440e+01
5	0.12	0.12	8.81	8.81	1.5791367e+02
6	2.20	2.20	11.02	11.02	2.4674011e+02
7	5.72	5.72	12.38	12.38	3.5530576e+02
8	11.67	11.67	7.82	7.82	4.8361062e+02
9	125.74	125.74	-	-	6.3165468e+02
10	86.56	86.56	-	-	7.9943796e+02

6.2 Example 2: Ordinary Differential Equation

Let us consider the ODE $u''+u+x=0$ in the domain $[0,1]$, with boundary conditions $u(0)=u(1)=0$. The exact solution is given by:

$$u_{exact}(x) = \frac{\sin x}{\sin 1} - x \tag{62}$$

The accuracy of each formulation is evaluated in terms of the L_2-norm, which in our case was taken in percent (%) using the formula:

$$L_2 = \left[\frac{\int_0^L (u_{calculated}-u_{exact})^2\,dx}{\int_0^L (u_{exact})^2\,dx}\right]^{\frac{1}{2}} \times 100\% \tag{63}$$

Using now a variable number of $n_{ele}=1,\ldots,10$ uniform elements that span the domain $[0,1]$, the L_2-norm is shown in Table 2.

Table 2. L_2-norm for several uniform discretizations

Number of elements (n_{ele})	L_2-norm in percent (%)			
	Galerkin method		Collocation method	
	Global	Local	Global	Local
1	3.0122811e-01	3.0122811e-01	1.9548847e+00	1.9548847e+00
2	3.5241821e-02	3.5241821e-02	1.2632632e-01	1.2632632e-01
3	8.8421658e-03	8.8421658e-03	2.5070791e-02	2.5070791e-02
4	3.1388530e-03	3.1388530e-03	7.9449369e-03	7.9449369e-03
5	1.3729196e-03	1.3729196e-03	3.2565510e-03	3.2565510e-03
6	6.9050132e-04	6.9050132e-04	1.5710803e-03	1.5710803e-03
7	3.8370598e-04	3.8370598e-04	8.4822380e-04	8.4822380e-04
8	2.2975322e-04	2.2975322e-04	4.9728673e-04	4.9728673e-04
9	1.4577665e-04	1.4577665e-04	3.1048506e-04	3.1048506e-04
10	9.6871369e-05	9.6871369e-05	2.0372396e-04	2.0372396e-04

7 Discussion

The existence of the original Theorem-1 would be sufficient to establish the equivalence between C^1-continuous cubic B-splines and cubic Hermite polynomials. Therefore, in principle, section 5 and section 6 could be omitted. Nevertheless, these two sections remain cited, for the sake of completeness and for the benefit of the reader, because only after their completion it was made possible to formulate Theorem-1. In other words, sections 5 and 6 were the source of inspiration for this novel theorem.

It is recognized that the numerical results are basic but were chosen because they possess closed-form analytical solutions, and thus they leave no room for doubt regarding the achieved accuracy. The interested reader may implement any other test case, for which (because of Theorem-1) he/she will find identical results for both formulations. It is worth mentioning that the coincidence of the numerical results between the two formulations was the earliest observation (approximately fifteen years ago) and the practical reason for seeking a theoretical explanation in terms of Theorem-1.

The present study is limited to one-dimensional problems using B-splines only, for which international research continues, [10], [11]. The application (or the modification) of Theorem-1 to two-dimensional problems is still an open issue.

8 Conclusions

It was theoretically shown that, for one-dimensional problems, the functional set being inherent in the global cubic B-spline approximation of C^1-continuity, is a linear transformation of the set of four conventional cubic Hermite polynomials involved per element. A generic closed-form expression was proposed for the transformation matrix, based on the length ratios of the adjacent elements at the interelement junctions. Numerical implementation of Galerkin and collocation methods, using both the B-spline and conventional Hermite finite elements, showed identical results of both approximation types in each separate method. Practically, this means that instead of implementing the subroutines of C^1-continuous cubic B-splines, it is equivalent to using piecewise-cubic Hermite elements, like those used in beam bending analysis.

References:

[1] Schoenberg I.J., Contributions to the problem of approximation of equidistant data by analytic functions. Part A. On the problem of smoothing or graduation. A first class of analytic approximation formulae, *Q Appl. Math*, Vol.4, No.1, 1946, pp. 45–99. https://doi.org/10.1090/qam/15914.

[2] Curry H.B., and Schoenberg I.J., On Pólya frequency functions IV: the fundamental spline functions and their limits, *Journal d'Analyse Mathématique*, Vol.17, No.1, 1966, pp. 71–107. https://doi.org/10.1007/BF02788653.

[3] De Boor C., *The method of projections as applied to the numerical solutions of two-point boundary value problems using cubic splines*, Ph.D. thesis, University of Michigan, 1966.

[4] De Boor C., On calculating with B-splines, *J. Approx. Theory*, Vol.6, No.1, 1972, pp. 50–62. https://doi.org/10.1016/0021-9045(72)90080-9.

[5] De Boor C., *A practical guide to splines*, Revised edition (first edition in 1978). Springer, 2001. ISBN: 978-0-387-95366-3.

[6] Höllig K., *Finite Element Methods with B-Splines*, SIAM, 2003. https://doi.org/10.1137/1.9780898717532.

[7] De Boor C., and Swartz B., Collocation at Gaussian points, *SIAM J. Numer. Anal.*, Vol.10, No.4, 1973, 582–606. https://doi.org/10.1137/0710052.

[8] Provatidis C.G., Finite element analysis of structures using C^1-continuous cubic B-splines or equivalent Hermite elements, *Journal of Structures*, Vol. 2014 (2014), Article ID 754561, 9 pages. https://doi.org/10.1155/2014/754561.

[9] Piegl L., Tiller W., *The NURBS Book*, 2nd edition, Springer, 1997. https://doi.org/10.1007/978-3-642-59223-2.

[10] Shumilov B.M., An efficient way of a non-Hermitian wavelet-based signal decomposition, *WSEAS Transactions on Signal Processing*, Vol.18, 2022, 25–36. https://doi.org/10.37394/232014.2022.18.4.

[11] Inkpé H.J.S., Uriel A., Aurélien G., Isogeometric Method for Least Squares Problem, *WSEAS Transactions on Mathematics*, Vol.23, 2024, 750–756. https://doi.org/10.37394/23206.2024.23.78.

Contribution of Individual Authors to the Creation of a Scientific Article (Ghostwriting Policy)

Christopher Provatidis conceived the main idea, performed all the calculations in MATLAB® R2020a environment, and wrote the entire manuscript.

Sources of Funding for Research Presented in a Scientific Article or Scientific Article Itself

No funding was received for conducting this study.

Conflict of Interest

The author has no conflicts to disclose.

APPENDICES

Appendix A: Matrices of Hermite element

For the Hermite element of length L_e, having the shape functions of Eq. (20), the analytical integration on the integrands involved in the mass matrix ($\mathbf{M}_e$) and stiffness matrix ($\mathbf{K}_e$), according to Eq. (7), lead to the following expressions:

$$\mathbf{M}_e = \frac{L_e}{420c^2}\begin{bmatrix} 156 & 22 & 54 & -13 \\ 22 & 4 & 13 & -3 \\ 54 & 13 & 156 & -22 \\ -13 & -3 & -22 & 4 \end{bmatrix} \quad \text{(A.1)}$$

and

$$\mathbf{K}_e = \frac{1}{L_e}\begin{bmatrix} 6/5 & 1/10 & -6/5 & 1/10 \\ 1/10 & 2/15 & -1/10 & -1/30 \\ -6/5 & -1/10 & 6/5 & -1/10 \\ 1/10 & -1/30 & -1/10 & 2/15 \end{bmatrix} = \frac{1}{30L_e}\begin{bmatrix} 36 & 3 & -36 & 3 \\ 3 & 4 & -3 & -1 \\ -36 & -3 & 36 & -3 \\ 3 & -1 & -3 & 4 \end{bmatrix} \quad \text{(A.2)}$$

Appendix B: Derivative at the free end ($x = L$)

We shall show that a zero derivative at the endpoint $x = L$ leads to equality of the two greatest coefficients.

Indeed, the derivative of a B-spline of degree p is given by the formula (see, Ref. [9]):

$$\frac{dN_{i,p}(x)}{dx} = p\left(\frac{N_{i,p-1}(x)}{u_{i+p}-u_i} - \frac{N_{i+1,p-1}(x)}{u_{i+p+1}-u_{i+1}}\right) \quad \text{(B.1)}$$

It is also known that among the n basis functions, only the last one becomes equal unity at the right endpoint whereby the others vanish, i.e.

$$N_n(L) = 1 \text{ and } N_i(L) = 0, i = 1,\ldots,n-1. \quad \text{(B.2)}$$

The latter happens to any degree; in our case we are interested in $p = 3$ and $p' = 2$.

Since the multiplicity is $\lambda = 2$ (double knots), within the utmost right B-spline element the $p+1$ nonzero basis functions will be $N_i(x)$ with $i = n-3,\ldots,n$ (for $p = 3$).

Setting in Eq. (B.1) the indices associated to the nearest-to-the-end element ($i = n-3,\ldots,n$), and also considering Eq. (B.2), we find that for the derivatives of the basis functions associated to the first two indices vanish (i.e., $N_{n-3,p} = N_{n-2,p} = 0$), while those associated to the next two which are the nearest control points to the end (at $x = L$) are characterized by equal and opposite derivatives, i.e.:

$$N'_{n-1}(L) = -N'_n(L). \quad \text{(B.3)}$$

It is left to the reader to prove that for the knot vector of Eq. (1), the positive value of the derivative in Eq. (B.3) equals 12 (i.e., $N'_{n-1}(1) = -12$ and $N'_n(1) = 12$) with $n = 10$.